Kumazawa, T., Nakajima, A., Ishiguro, T., Jiuxin, Z., Tanaharu, T., Nishitani, H., Inoue, Y., Harada, S., Hayasaka, I. and Tagawa, Y. (2009): Collaborative work on evaluation of ovarian toxicity 15) Two- or four-week repeated-dose studies and fertility study of bromocriptine in female rats. J. Toxicol. Sci., **34** (Special Issue I), SP157-SP165.

Muskhelishvili, L., Wingard, S.K. and Latendresse, J.R. (2005): Proliferating cell nuclear antigen - A marker for ovarian follicle counts. Toxicol. Pathol., **33**, 365-368.

Nozaki, Y., Furubo, E., Matsuno, T., Fukui, R., Kizawa, K., Kozaki, T. and Sanzen, T. (2009): Collaborative work on evaluation of ovarian toxicity. 6) Two- or four-week repeated-dose studies and fertility study of cisplatin in female rats. J. Toxicol. Sci., **34** (Special Issue I), SP73-SP81.

Ohtake, S., Fukui, M. and Hisada, S. (2009): Collaborative work on evaluation of ovarian toxicity 1) Effects of 2- or 4- week repeated-dose administration and fertility studies with medroxyprogesterone acetate female in rats. J. Toxicol. Sci., **34** (Special Issue I), SP23-SP29.

Pedersen, T. and Peters, H. (1968): Proposal for a classification of oocytes and follicles in the mouse ovary. J. Reprod. Fert., **17**, 555-557

Regan, K.S., Cline, J.M., Creasy, D., Davis, B., Foley, G.L., Lanning, L., Latendresse, J.R., Makris, S., Morton, D., Rehm, S. and Stebbins, K. (2005): STP Position Paper: Ovarian follicular counting in the assessment of rodent reproductive toxicity. Toxicol. Pathol., **33**, 409-412.

Sakurada, Y., Kudo, S., Iwasaki, S., Miyata, Y., Nishi, M. and Masumoto, Y. (2009): Collaborative work on evaluation of ovarian toxicity 5) Two- or four-week repeated-dose studies and fertility study of busulfan in female rats. J. Toxicol. Sci., **34** (Special Issue I), SP65-SP72.

Sato, M., Shiozawa, K., Uesugi, T., Hiromatsu, R., Fukuda, M., Kitaura, K., Minami, T. and Matsumoto, S. (2009): Collaborative work on evaluation of ovarian toxicity 7) Effects of 2- or 4- week repeated dose studies and fertility study of cyclophosphamide in female rats. J. Toxicol. Sci., **34** (Special Issue I), SP83-SP89.

Sato, N., Uchida, K., Nakajima, M., Watanabe, A. and Kohira, T. (2009): Collaborative work on evaluation of ovarian toxicity 13) Two- or four-week repeated dose studies and fertility study of PPAR α/γ dual agonist in female rats. J. Toxicol. Sci., **34** (Special Issue I), SP137-SP146.

Shibayama, H., Kotera, K., Shinoda, Y., Hanada, T., Kajihara, T., Ueda, M., Tamura, H., Ishibashi, S., Yamashita, Y. and Ochi, S. (2009): Collaborative work on evaluation of ovarian toxicity 14) Two- or four-week repeated-dose studies and fertility study of atrazine in female rats. J. Toxicol. Sci., **34** (Special Issue I), SP147-SP155.

Shirai, M., Sakurai, K., Saitoh, W., Matuyama, T., Teranishi, M., Furukawa, T., Sanbuissho, A. and Manabe, S. (2009): Collaborative work on evaluation of ovarian toxicity 8) Two- or four-week repeated-dose studies and fertility study of Anastrozole in female rats. J. Toxicol. Sci., **34** (Special Issue I), SP91-SP99.

Shirota, M., Watanabe, G., Taya, K. and Sasamoto, S. (1998): Effect of indomethacin on the selective release of follicle-stimulating hormone during the period of ovulation in the rat. J. Vet. Med. Sci., **60**, 1059-1065.

Takai, R., Hayashi, S., Kiyokawa, J., Iwata, Y., Matsuo, S., Suzuki, M., Mizoguchi, K., Chiba, S. and Deki, T. (2009): Collaborative work on evaluation of ovarian toxicity 10) Two- or four-week repeated dose studies and fertility study of di-(2-ethylhexyl) phthalate (DEHP) in female rats. J. Toxicol. Sci., **34** (Special Issue I), SP111-SP119.

Tamura, T., Yokoi, R., Okuhara, Y., Harada, C., Terashima, Y., Hayashi, M., Nagasawa, T., Onozato, T, Kobayashi, K., Kuroda, J. and Kusama, H. (2009): Collaborative work on evaluation of ovarian toxicity 2) Two- or four-week repeated dose studies and fertility study of mifepristone in female rats. J. Toxicol. Sci., **34** (Special Issue I), SP31-SP42.

Tsubota, K., Kushima, K., Yamauchi, K., Matsuo, S., Saegusa, T., Ito, S., Fujiwara, M., Matsumoto, M., Nakatsuji, S., Seki, J. and Oishi, Y. (2009): Collaborative work on evaluation of ovarian toxicity 12) Effects of 2- or 4-week repeated dose studies and fertility study of indomethacin in female rats. J. Toxicol. Sci., **34** (Special Issue I), SP129-SP136.

Tsujioka, S., Ban, Y., Wise, L.D., Tsuchiya, T., Sato, T., Matsue, K., Ikeda, T., Sasaki, M. and Nishikibe, M. (2009): Collaborative work on evaluation of ovarian toxicity 3) Effects of 2- or 4-week repeated dose toxicity and fertility studies with tamoxifen in female rats. J. Toxicol. Sci., **34** (Special Issue I), SP43-SP51.

Wato, E., Asahiyama, M., Suzuki, A., Funyu, S. and Amano, Y. (2009): Collaborative work on evaluation of ovarian toxicity 9) Effects of 2- or 4-week repeated dose studies and fertility study of di(2-ethylhexyl)adipate (DEHA) in female rats. J. Toxicol. Sci., **34** (Special Issue I), SP101-SP109.

Yoshida, M., Sanbuissho, A., Hisada, S., Takahashi, M., Ohno, Y. and Nishikawa, A. (2009): Morphological characterization of the ovary under normal cycling in rats and its viewpoints of ovarian toxicity detection. J. Toxicol. Sci., **34** (Special Issue I), SP189-SP197.

The Journal of Toxicological Sciences (J. Toxicol. Sci.)
Vol.34, Special Issue I, SP189-SP197, 2009

Morphological characterization of the ovary under normal cycling in rats and its viewpoints of ovarian toxicity detection

Midori Yoshida[1], Atsushi Sanbuissyo[2], Shigeru Hisada[3], Michihito Takahashi[4], Yasuo Ohno[5] and Akiyoshi Nishikawa[1]

[1]Division of Pathology, Biology Safety Research Center, National Institute of Health Sciences, 1-18-1 Kamiyoga, Setagaya-ku, Tokyo 158-8501, Japan
[2]Medical Safety Research Laboratories, R & D Division, Daiichi-Sankyo Co., Ltd., 717 Horikoshi, Fukuroi, Shizuoka 437-0065, Japan
[3]Safety Research Department, Aska Pharmaceutical Co. Ltd., 1604 Shimosakunobe, Taktsu-ku, Kawasaki 213-8522, Japan
[4]Pathology Peer Review Center, 3-45-11 Uehara, Shibuya-ku, Tokyo 151-0064, Japan
[5]National Institute of Health Sciences, 1-18-1 Kamiyoga, Setagaya-ku, Tokyo 158-8501, Japan

(Received December 10, 2008)

ABSTRACT — Identification of ovarian toxicity is very important for safety assessment of drugs and other environmental chemicals. The detection of interference with ovarian function is very hard without a thorough understanding of the normal ovarian morphology based on reproductive physiology. The focus of the present study was therefore a practical analysis in each stage of the estrous cycles using ovaries obtained from 143 rats demonstrating normal cycling. Transversely dissected maximum areas in the ovaries were examined microscopically for the two major features, follicles and corpora lutea (CL). Classification of growing follicles was in reference to Pedersen and Peters (1968), and functionally divided into follicular stimulating hormone (FSH)-independent and dependent categories. The former, small and medium-sized follicles, respectively primordial/primary and preantral follicles, could be readily detected by immunohistochemical staining for proliferating cell nuclear antigen (PCNA). The large antral and Graafian follicles and large sized atretic follicles showed sequential changes depending on the estrous cycle stage. CL could be divided into currently and previously formed examples. Currently formed CL underwent remarkable changes in their appearance with the cycle, reflecting ovulation and progesterone production. Thus morphological analysis that is synchronized the large antral follicle changes with recently formed CL ones allows the ovary to be classified into the each estrous cycle stage. Morphological deviation from any synchronized combination provides a first pointer of ovarian toxicity. PCNA immunohistochemical staining is also useful to detect small follicles.

Key words: Estrous cycle, Morphology, Ovarian toxicity, Rat

INTRODUCTION

Detection of ovarian toxicity in preclinical studies is very important for safety assessment of drugs and chemicals, because oocytes have no regenerative ability, and any abnormalities in the ovaries may be directly linked to impairment of female reproductive capacity. The U.S. Environmental Protection Agency (EPA), U.S. Food and Drug Administration (FDA) and the Organization for Economic Cooperation and Development (OECD) recommended qualitative and quantitative evaluation of primordial follicles in the ovary for regulatory guidelines for 2-generation reproductive toxicity studies (U.S. EPA, 1998; U.S. FDA, 2000; OECD, 2001). The ovary has a complicated structure and its appearance changes with the estrous cycle, so that detection of interference with ovarian function requires a comprehensive understanding of the normal variation in ovarian morphology. In particular, the growth of follicles and corpora lutea (CL) and their regression, as well as knowledge on the hypothalmo-pituitary-gonadal axis control system are crucial. Quantitative follicular analysis using serial sections is accepted

Correspondence: Midori Yoshida (E-mail: midoriy@nihs.go.jp)

for assessment of both biological reproduction and toxicology (Bolon *et al.*, 1997; U.S. EPA, 1998; Meredith *et al.*, 1999; OECD, 2001; U.S. FDA, 2000), although the approach is very laborious and time-consuming.

According to the guideline of non-clinical safety studies, the completion of a female fertility study is required prior to the enrollment of women with childbearing potential in phase I clinical trials conducted in Japan. On the other hand, the completion is required prior to phase III clinical trials only in the United States and the European Union. Currently, the ICM M3 program to harmonize these regional differences is progressing (The ICH Steering Committee to the regulatory authorities of the three ICH regions (the European Union, Japan and USA), 2008). For this harmonization, collaboration among the members of the Japan Pharmaceutical Manufacturers Association was organized to conduct validation studies (Sanbuissho *et al.*, 2009). In the validation studies, any improvement to increase attention to toxicity to the female reproductive organs or many conventional guides or references to consistent, reliable and cost-effective methods are required using rat repeated toxicity studies. Recently, immunohistochemical staining of proliferating cell nuclear antigen (PCNA) has been accepted as a useful aid to making ovarian follicle counts, particularly for primordial and primary follicles (Muskhelishvili *et al.*, 2005; Picut *et al.*, 2008). The Society of Toxicologic Pathology (STP) ovary evaluation working group has published a position paper on histopathological approaches for the assessment of rodent reproductive toxicity, and recommended qualitative evaluation of the ovary as the first-tier assessment (Regan *et al.*, 2005). The OECD (2008) is preparing a guidance document for histopathological evaluation with endocrine and reproductive tests to detect chemicals with hormonal potential, including estrogens and antiestrogens. Westwood (2008) has just produced a good practical histological guide of the female reproductive tract in normal cycling rats. However, there is still only limited information on ovarian morphology of relevance to toxicological assessment. The main purpose of the present study was therefore to provide a practical guide of ovarian morphology in rats undergoing normal cycling. In addition, several morphological and methodological points for detection of ovarian toxicity are highlighted.

MATERIALS AND METHODS

Animals

Forty-eight Fischer344 DuCrlCrlj (Fischer) female rats aged 3 months and 92 Crlj:DON (Donryu) female rats aged 3 or 4 months purchased from Charles River Laboratories Japan, Inc. (Kanagawa, Japan) were available for the present study. The animals were maintained in an air-conditioned animal rooms under constant conditions of 24 ± 2°C and 55 ± 10% humidity with a 12-hr light/dark cycle (lighting from 8:00 to 20:00; dark, 20:00 to 8:00), housed 3 or 4 rats per cage, and allowed free access to commercial rodent chow, CRF-1 (Oriental yeast Co., Ltd., Kanagawa, Japan) and drinking water throughout. The Donryu strain rats were checked for estrous cyclicity by vaginal cytology during 9:00-10:00am throughout the study. Animal care and use followed the guidelines for the Care and Use of Laboratory Animals in the National Institute of Health Sciences.

Histology

At necropsy, all animals were euthanized under deep ether anesthesia in the morning. After exsanguination, the ovaries were removed from attached tissues such as ovarian bursa and oviduct, weighed and fixed in 10 vol% neutral buffered formalin. At dissection, the bilateral ovaries were transversally halved to examine maximum areas microscopically. The uterine horn and the vagina also were fixed to allow confirmation of the estrous cycle stage. All of the organs were embedded in paraffin, sectioned at 4 μm and stained with hematoxylin and eosin (HE). All the animals used in the present study showed a normal estrous cycle and the estrous cycle stages at necropsy were determined by vaginal cytology and morphological features in the uterus and the vagina with reference to previous studies (OECD, 2008; Westwood, 2008; Yuan and Foley, 2002).

Immunohistochemistry

Serial sections in the ovaries were incubated with anti-PCNA antibody (Dako Japan, Kyoto, Japan) to find small follicles such as primordial and primary follicles or to distinguish growing follicles as reported by Muskhelishvili *et al.* (2005).

Classification of follicles

In the present study, we applied Pedersen's follicular classification in rodents (Pedersen and Peters, 1968), featuring division into 3 main categories, i.e., small, medium and large corresponding to primordial or primary, preantral, and antral or Graafian follicles, respectively (Table 1). These were further subdivided into 8 types (Types 1 to 8) according to the morphological appearance and follicular size. The classification was established for mouse ovary, but application to the rat or hamster ovary has been recommended (Greenwald and Roy, 1994). In the present

Table 1. Classification of growing follicles

This article	Pedersen and Peters (1968)	Characteristics and Synonyms
Small	Small, Type 1a to 3a	Primordial and primary follicles. Type 3a follicle is a primary follicle with complete ring surrounding small oocyte.
Medium	Medium, Type 3b to 5a	Type 3b follicle is a primary follicle with complete ring surrounding growing oocyte. Secondary follicles and preantral follicles less than 70 μ on the largest cross-section.
Large	Large, Type 5b to 8	Type 5b follicle is preantral one with a fully grown ooctyes surrounded by many layers of granulosa cells. Type 6 follicle is a small antral one with a large oocyte with many layers of granulosa cells and scattered areas of fluid. Type 7 follicle is a antral one with single cavity containing follicle fluid. The cumulus oohorus has formed, but not be formed the stalk. Type 8 follicle is a large antral follicle with a single cavity with follicle fluid and a well-formed cumulus stalk. Type 8 follicle is also termed as Graafian or preovulatory follicles.

study, large follicles without oocytes in the sections were distinguished by morphological features of the granulosa cells and the thickness of the theca cell layer as far as possible. Follicles with apoptotic cells in the granulosa cell layer or degeneration of oocytes were judged as atresia. Atretic follicles were also classified into small, medium or large sized. If necessary, more detailed descriptions based on the follicle size in Pedersen's classification were added.

Classification of CL

CL were divided into currently formed CL and previously formed ones. Currently formed CL, which are also termed as most recently formed or new CL, are defined within one estrous cycle after ovulation. The previously formed CL, which are also termed as old CL, remain in the ovary throughout several estrous cycles before their complete dissolution. In currently formed CL, the ones observed at estrus when ovulation occurred early in the morning were defined as newly formed CL in this article.

Counts of Follicles and newly formed CL

The numbers of each type of follicle, atretic follicles and newly formed CL were counted in unilateral ovaries in F344 rats. Small and medium follicles were recognized on the basis of PCNA positive nuclei. Large follicles and CL were identified primarily in HE-stained samples. Separation was made into each estrous cycle stage. Statistical analysis was with ANOVA and P Values less than 0.05 were considered to be significant.

RESULTS

Small and medium follicles were distributed unevenly throughout the ovary, and they were easily detectable with PCNA immunohistochemical staining (Fig. 1). Small follicles were occasionally aggregated in the cortex. The estrous cycle did not affect their distribution or number. Typical atretic follicles were usually easy to detect at low magnification in HE stained sections. Higher magnification observation after HE staining was often necessary for detection of atretic follicles at early stages, focusing on apoptotic cells in the granulosa cell layer in early stages with other granulosa cells still positive for PCNA (Fig. 2).

Histological characteristics of each estrous cycle stage were as follows:

Proestrus (Fig. 3)

Follicles

Large follicles such as Graafian or Type 8 follicles in Pedersen's classification were evident at this stage. The large follicles Type 8 were located in surface area of the ovary (Figs. 3A-B). Their granulosa cells were cuboidal and/or polygonal, resembling the luteal cells at estrus (Figs. 3C-D). Most large follicles without the cumulus oophorus could be recognized by a thickened theca cell layer or cuboidal or polygonal granulosa cells (Figs. 3E-F). Large follicles Type 7 and some of Type 6 were atretic.

CL

Currently formed CL were starting degenerative processes characterized by vacuoles in cytoplasm, and increased apoptotic cells. Necrosis in the central parts was sometimes observed (Figs. 3G-H). Fibrous tissue proliferation was noted in previously formed CL.

Estrus (Fig. 4)

Follicles

There was a lack of large follicles such as Type 7 or 8. Although distinction of large follicles from degenerated large follicles was sometimes difficult at lower magnification, apoptotic granulosa cells in the degenerated large follicles were recognized them as atretic follicles (Fig. 4C). A number of large follicles of Type 6 were observed.

CL

Newly formed CL were characteristically observed as currently formed ones after ovulation (Figs. 4A-D). They were composed of basophilic, small and spindle-shaped luteal cells, positive for PCNA antibody binding (Figs. 4B-C). In addition, the newly formed CL were easily and clearly distinguishable from the large follicles by angiogenesis between the luteal cells and the break down of the basement membrane between the granulosa cell layer and the theca cell layer (Fig. 4D). Previously formed CL had a similar size as those at proesturs, but degenerative processes including fibrosis were more advanced (Figs. 4E-F).

Metestrus (Fig. 5)

Follicles

There were no large follicles of Type 8, but many large follicles Type 7 were growing (Fig. 5F). Atretic follicles were observed in all types of follicles at a constant rate.

CL

Currently formed CL were characteristically observed. They were increased in size compared to those at estrus, but smaller than those at diestrus (Figs. 5B-D). The luteal cells had still basophilic but not foamy cytoplasm with large nuclei and nucleoli prominent (Fig. 5C). The CL sometimes contained fluid-filled central cavities of various sizes (Figs. 5G-H). PCNA levels in the luteal cells were lower than in that at estrus (Fig. 5I). Previously formed CL demonstrated advanced fibrosis, but their sizes were still similar to those of currently formed examples.

Diestrus (Fig. 6)

Follicles

Large follicles Types 7 and 8 were increased in number, but the latter were smaller than at proestrus (Fig. 6A). Atretic follicles were observed in all types at a constant rate.

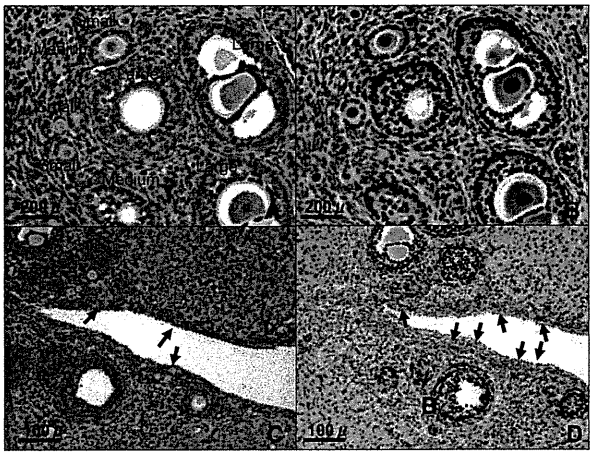

Fig. 1. Classification of follicles. **A**, Small follicles (small), medium follicles (medium), and large follicles are shown. **B**, Immunohistochemical staining for PCNA in a serial section to A. All oocytes and most granulosa cells are positive for PCNA. **C**, Small follicles (arrows) are not distributed uniformly and their identification with HE staining is difficult. **D**, Serial section to C. Note that small follicles (arrows) are easy to detect with PCNA immunohistochemical staining.

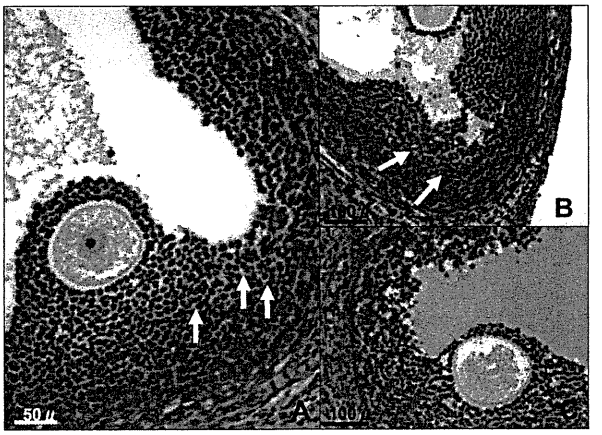

Fig. 2. Various types of atretic follicles. **A**, Early stage. A few apoptotic cells are apparent in the granulosa cell layer in a large follicle (arrows). **B**, Apoptotic cells are scattered in the granulosa cell layer (arrows). **C**, A number of apoptotic cells are present in the lumen and the granulosa cell layer. A-C, HE staining.

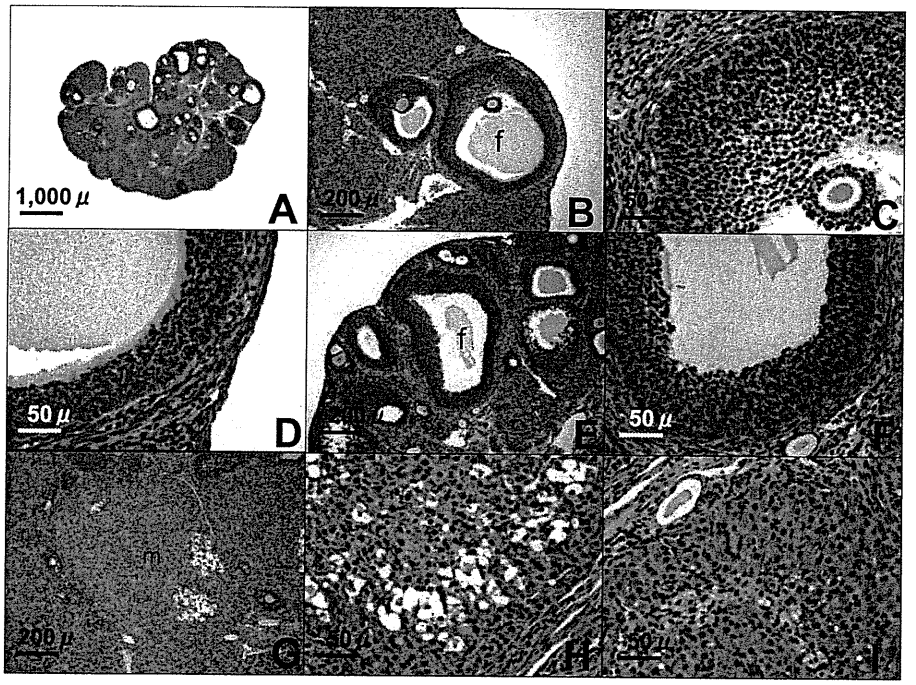

Fig. 3. The ovary at proestrus. **A**, Low-magnification. Large follicles are evident. **B**, A large follicle of Type 8 (f). **C**, Higher magnification of B. Cumulus oophorus formation. **D**, The same large follicle as B. The granulosa cells are round to cuboidal or polygonal in shape, indicating a luteinizing function **E**, A large follicle without cumulus oophorus (f). **F**, Higher magnification of E. Polygonal granulosa cells without apoptotic cells have characteristic of a large follicle Type 8. **G**, A currently formed corpus luteum. **H**, The corpus luteum contains vacuolated, degenerating and necrotic luteal cells in the central portion with some fibrous tissue. **I**, A previously formed corpus luteum. Note proliferation of fibrous tissue. A-I, HE staining.

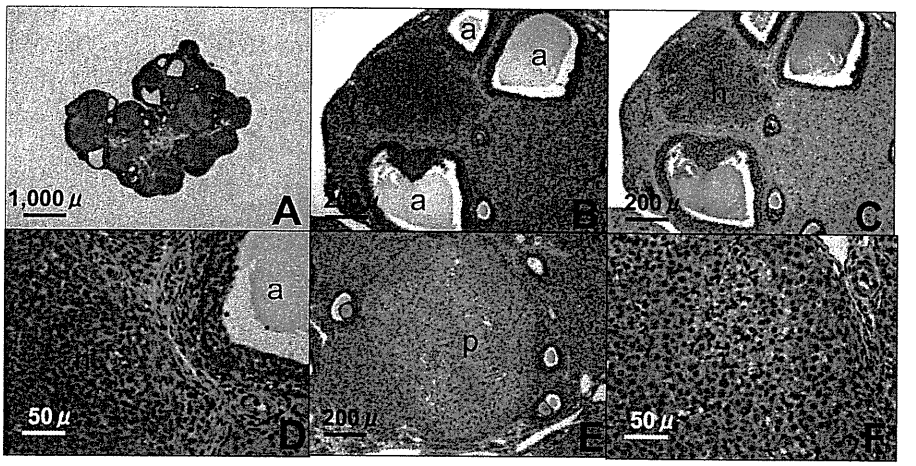

Fig. 4. The ovary at estrus. **A**, Low-magnification. **B**, A currently formed corpus luteum (n) is recognized as a newly formed one at this stage. Large sized atretic follicles are also observed (a). **C**, PCNA immunohistochemical staining of a serial section to B. A newly formed corpus luteum is strongly positive. **D**, Higher magnification of B. Spindle-shaped basophilic luteal cells and capillary formation are observed in a newly formed corpus luteum (n). A large sized atretic follicle is also detected at right upper part (a). **E**, Previously formed corpus luteum (p) of still large size. **F**, Higher magnification of E. Vacuolated and apoptotic cells are apparent. A, B, D-F, HE staining; C, PCNA immunohistochemical staining.

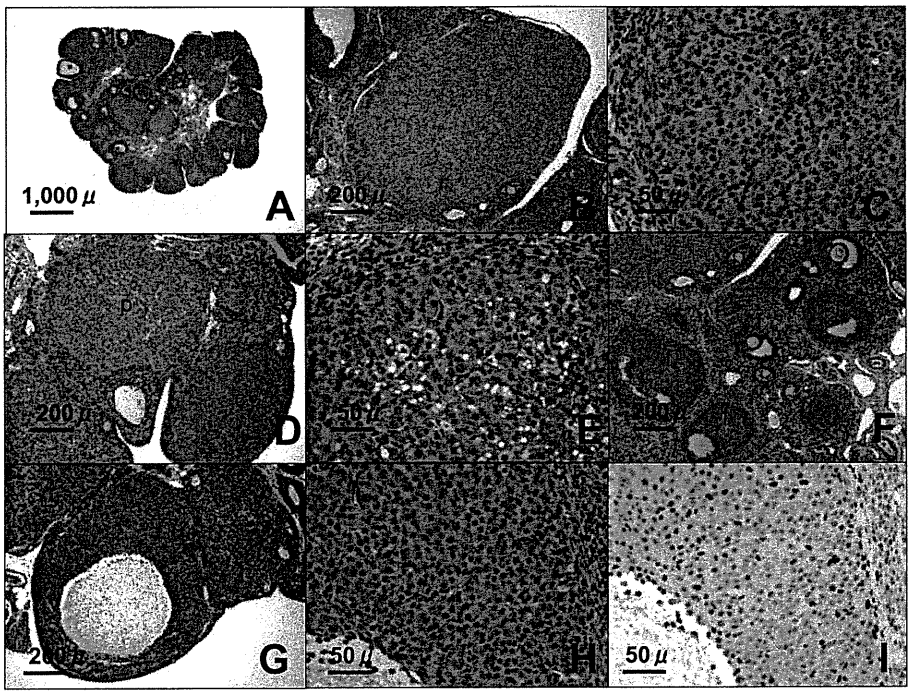

Fig. 5. The ovary at metestrus. **A**, Low-magnification. **B**, A currently formed corpus luteum. **C**, Higher magnification of B. The basophilic luteal cells sometimes exhibit prominent nucleoli. **D**, Currently formed (c) and previously formed (p) CL. Currently formed CL are still smaller than previously formed ones. **E**, A previously formed corpus luteum with fibrous tissue infiltration. **F**, Large follicles of Type 7 (f) appear at this stage. **G**, Currently formed copus luteum with a cavity. **H**, Higher magnification of G. Morphology of the luteal cells is very similar to 5C. **I**, PCNA immunohistochemical staining of a serial section to 5H. A-H, HE staining; I, PCNA immunohistochemical staining.

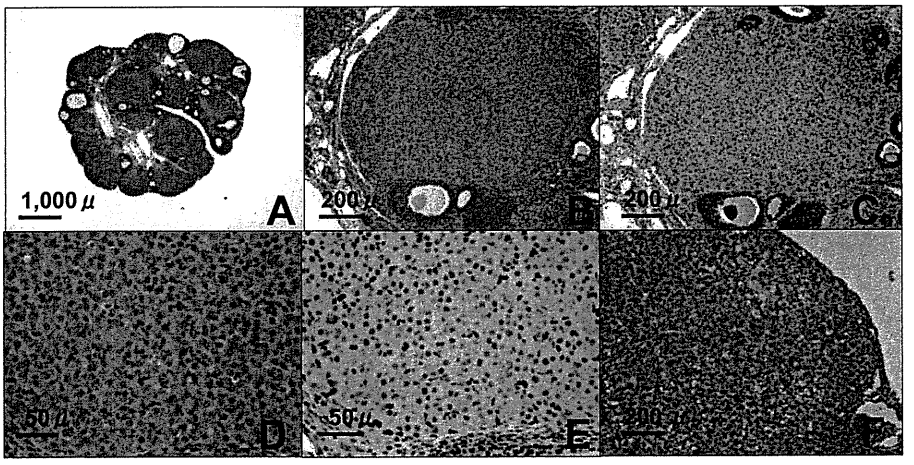

Fig. 6. The ovary at diestrus. **A**, Low-magnification **B**, A currently formed corpus luteum. **C**, A serial section of A immunohistochemically stained with PCNA antibody. **D**, Higher magnification of B. It is larger than at metestrus and the cytoplasm of their component cells is foamy and eosinophilic. **E**, Higher magnification of C. Most luteal cells are negative for PCNA, in contrast to fibrous tissue including fibroblasts or lymphoid cells. **F**, A previously formed corpus luteum with vacuolated luteal cells and fibrous tissue infiltration. A, B, D, F, HE staining. C, E, PCNA immunohistochemical staining.

CL

Currently formed CL had attained the maximum size (Figs. 6A-C). The luteal cells had foamy eosinophilic cytoplasm (Fig. 6D). Most luteal cells were negative for PCNA (Fig. 6E), and fibrous tissue were sometimes detected in the center of CL. Previously formed CL were vacuolated and fibrous tissue infiltration was advanced (Fig. 6F).

The average numbers of follicles and newly formed CL are shown in Table 2. Whereas the numbers of all follicular types and newly formed CL varied, the counts indicated some tendencies as follows: 1) small and medium follicles were found at constant ratios in all stages; 2) large follicles of Type 8 appeared at diestrus and reached a peak in proestrus; and 3) newly formed CL were found only in the estrus stage.

DISCUSSION

The present study demonstrated that the synchronized combination of morphological findings in large follicles, which are follicle stimulating hormone (FSH)-dependent (Greenwald and Roy, 1994), and currently formed CL is allowed as the ovary reliable clarification of each estrous cycle stage. In particular, classification of CL into 2 types appears very useful for staging. There were no morphological differences in either follicles or CLs between F344 and Donryu rats.

Our results for the estrous cycle are similar to those reported previously except for the detailed description of follicular changes (OECD, 2008; Westwood, 2008). In brief, in **proestrus**, the most characteristic feature is the presence of large follicles of Type 8 (Graafian follicles). In addition, cytoplasmic similarity of granulosa cells to luteal cells is characteristic of the Type 8 follicle. The increase in atretic change of Type 7 follicles indicated withdrawal of this type of follicle on the morning after ovulation. While currently formed CL at proestrus resembled those at diestrus, they appeared to be much more regressive. **Estrus** is the easiest stage to recognize due to newly formed CL. Confirmation of angiogenesis in CL in this stage is important to avoid misdiagnosing them from the edge of the Graafian follicles. A lack of large follicles of Types 7 and 8 is also a feature at estrus. Many large follicles of Type 6 might reflect the start of growing large follicles toward next ovulation (Watanabe *et al.*, 1990; Freeman, 2006). **At metestrus**, currently formed CL typicaly had luteal cells with basophilia and prominent nucleoli. This morphology might reflect progesterone production in rats classified into an ultrashort CL species (Freeman, 2006; Stouffer, 2006). **At diestrus,** currently formed CL were still characteristic. They reached the maximum size and contained luteal cells with eosinophilic and foamy cytoplasm. CL are not able to produce active progesterone at this stage (Watanabe *et al.*, 1990; Freeman, 2006).

CLs with cavities were encountered at metestrus in the present study. Their interpretation differs between OECD (2008) and Westwood (2008). Whereas OECD diagnoses them as ovarian luteal cysts which failed ovulation but undergoing luteinization of Graafian follicles in young adult rats (2008), Westwood described them as CL still containing occasional central fluid-filled cavities (2008). In domestic animals, CL with cavities have been accepted not to be confused with cystic follicles or luteinized cysts (Kenndey and Miller, 1993). On the other hand, the distinc-

Table 2. Follicular and newly formed CL counts per unilateral ovary (a) in F344 rats

	Estrous cycle			
Follicle/CL	Proestrus	Estrus	Metestrus	Diestrus
No. of rats examined	13	11	12	12
Follicles				
Small	15.9 ± 2.5 (b)	15.8 ± 3.3	17.0 ± 2.0	20.4 ± 4.4
Medium	2.2 ± 0.5	2.2 ± 0.5	2.0 ± 0.5	2.7 ± 0.4
Large (c)	16.7 ± 1.7	20.9 ± 0.1	18.0 ± 1.4	18.8 ± 2.2
Type 8	2.5 ± 0.3	0	0	0.8 ± 0.3
Atresia	10.8 ± 1.1	8.5 ± 1.4	11.9 ± 1.9	14.5 ± 1.6
CL				
Newly formed	0	1.6 ± 0.4	0	0

(a), the transverse section dissected to obtained maximum cut surface
(b), mean ± S.D.
(c), Including Type 8 follicles

tion between CL with cavity and luteinized cyst is sometimes difficult in rodents, multiovulated species. There are various description of similar morphology showing luteal tissue with cavity, such as CL containing cavities (Westwood, 2008), luteal cyst (OECD, 2008) or cystic CL (Yuan and Foley, 2002). In general, luteinized cysts are easy to distinguish from cystic follicles, which are very large atretic follicles and reflect impair of large follicle growth. They are caused by many chemicals and hormonal disturbances (Bogovich, 1991; Røste *et al.*, 2001; Baravalle *et al.*, 2006). In typical luteinized cyst arising from failure of ovulation and undergoing luteinization, the luteinized cells with angiogenesis formation are found in a thin cell layer or uneven distributed in crescent area in cows (Kenndey and Miller, 1993) and rats (Tamura *et al.*, 2009). The rupture of follicles at ovulation is mainly controlled by progesterone and prostaglandin, and disruptions of these hormones induce unruptured follicles with or without luteinization or formation of luteinized cysts (Davis *et al.*, 1999; Gaytán *et al.*, 2003; Shirota *et al.*, 1998; Tamura *et al.*, 2009; Tsubota *et al.*, 2009; Yuan and Foley, 2002). The CL containing small cavities seems to be normal range in normal cycling rats, because the cavity will be replaced to fibrous tissues next day, at diestrus. However, the toxicological significance of CL with cavities remains to be fully undetermined. We should pay attention an increase of CL-containing cavities in treated groups. Further investigation or information is required. Sequential vaginal cytology might be very informative to check ovulation.

Detection of damage to small follicles is very important for detection of ovarian toxicity in preclinical studies. Small follicle counts using single ovarian sections are challenging and evaluation may be misleading (Meredith *et al.*, 1999; Bolon *et al.*, 1997). However, FSH-independent small and medium follicles (Greenwald and Roy, 1994) were observed in all sections examined in the present study and at a constant rate with the estrous cycle stage. The result indicates that lack or only a few visible small follicles in a single ovarian section might give a pointer to alarm for small follicular damage. In addition, PCNA immunohistochemical staining and microscopic observation of bilateral ovaries are helpful to increase the reliability of detection. The STP Ovarian evaluation workshop group (Regan *et al.*, 2005) recommended a qualitative morphological approach for ovarian sections by toxicologic pathologists familiar with normal reproductive cycle as the first tier approach for detection of ovarian toxicity.

In conclusion, the present results demonstrate that ovarian morphology are allowed each estrous cycle stage by combination of morphologic changes in large follicles and CL undergoing development and/or regression (Fig. 7). In the classification of CL into 2 categories, morphological changes in currently formed CL appear particularly useful for staging. In addition, a single ovarian section might be sufficient for analyzing each estrous stage. Our results indicate that any morphological deviation in follicles and CL from the synchronized combination might be the first indicator of ovarian toxicity. PCNA immunohistochemical staining is useful to detect small follicles. Vaginal cytology is also informative for detection of endocrinological condition.

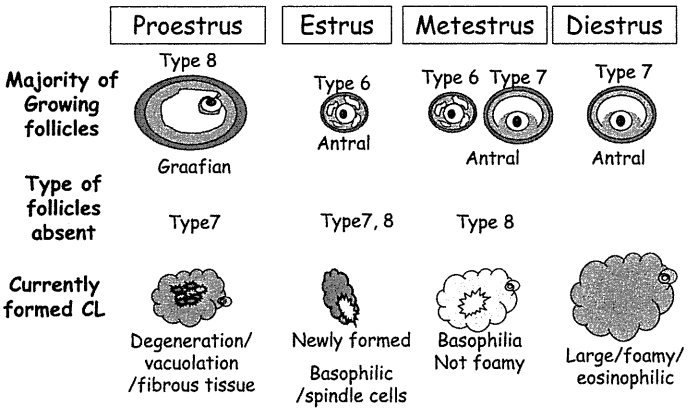

Fig. 7. A scheme for combination of morphologic features in follicles and CL at each estrous cycle in rats. The classification of follicles was referred to Pedersen and Peters (1968).

REFERENCES

Baravalle, C., Salvetti, N.R., Mira, G.A., Pezzone, N. and Ortega, H.H. (2006): Microscopic characterization of follicular structures in letrozole-induced polycystic ovarian syndrome in the rat. Arch. Med. Res., **37**, 830-839.

Bogovich, K. (1991): Induction of ovarian follicular cysts in the pregnant rat by human chorionic gonadotropin. Biol. Reprod., **45**, 34-42.

Bolon, B., Bucci, T.J., Warbritton, A.R., Chen, J.J., Mattison, D.R. and Heindel, J.J. (1997): Differential follicle counts as a screen for chemically induced ovarian toxicity in mice: results from continuous breeding bioassays. Fundam. Appl. Toxicol., **39**, 1-10.

Davis, B.J., Lennard, D.E., Lee, C.A., Tiano, H.F., Morham, S.G., Wetsel, W.C. and Langenbach, R. (1999): Anovulation in cyclooxygenase-2-deficient mice is restored by prostaglandin E2 and interleukin-1beta. Endocrinology, **140**, 2685-95.

Freeman, M.E. (2006): Neuroenodcrine control of the ovarian cycle of the rat, In the Physiology of Reproduction, Third Edition (Knobil, E., Neill, J.D. eds.) pp.2327-2388, Raven Press Ltd., New York.

Gaytán, F., Bellido, C., Gaytán, M., Morales, C. and Sánchez-Criado, J.E. (2003): Differential effects of RU486 and indomethacin on follicle rupture during the ovulatory process in the rat. Biol. Reprod., **69**, 99-105.

Greenwald, G.S. and Roy, S.K. (1994): Follicular development and its control. In The Physiology of Reproduction, Second Edition (Knobil, E., Neill, J.D. eds.) pp.629-724, Raven Press Ltd., New York.

Kennedy, P.C. and Miller, R.B. (1993): The female genital system. In Pathology of Domestic Animals. Fourth Edition. (Jubb, K. V. F., Kennedy, P. C., Palmer, N. eds.) pp.349-470, Academic Press, San Diego.

Meredith, S., Dudenhoeffer, G. and Jackson, K. (1999): Single-section counting error when distinguishing between primordial and early primary follicles in sections of rat ovary of different thickness. J. Reprod. Fertil., **117**, 339-343.

Muskhelishvili, L., Wingard, S.K. and Latendresse, J.R. (2005): Proliferating cell nuclear antigen--A marker for ovarian follicle counts. Toxicol. Pathol., **33**, 365-368.

Organization of Economic Cooperation and Development (2001): Proposal for updating Guideline 416: two generation reproduction toxicity study. In OECD Guideline for Testing of Chemicals, pp. 1-13. OECD, Paris.

Organization of Economic Cooperation and Development (OECD) (2008): Draft Guidance and Review Documents/Monographs, Guidance Document for Histopathologic Evaluation of Endocrine and Reproductive Tests. Part 3: Female reproductive system. http://www.oecd.org/document/12/0,3343,en_2649_34377_1898188_1_1_1_1,00.html

Pedersen, T. and Peters, H. (1968): Proposal for a classification of oocytes and follicles in the mouse ovary. J. Reprod. Fertil., **17**, 555-557.

Picut, C.A., Swanson, C.L, Scully, K.L., Roseman, V.C., Parder, R.F. and Remick, A.K. (2008): Ovarian follicle counts using proliferating cell nuclear antigen (PCNA) and semi-automated image analysis in rats. Toxicol. Pathol., **36**, 674-679.

Regan, K.S., Cline, J.M., Creasy, D., Davis, B., Foley, G.L., Lanning, L., Latendresse, J.R., Makris, S., Morton, D., Rehm, S., Stebbins, K. and STP Ovary Evaluation Working Group (2005): STP Position Paper: Ovarian follicular counting in the assessment of rodent reproductive toxicity. Toxicol. Pathol., **33**, 409-412.

Røste, L.S., Taubøll, E., Berner, A., Isojärvi, J.I.T. and Gjerstad, L. (2001): Valproate, but not lamotrigine, induces ovarian morphological changes in Wistar rats. Exp. Toxicol. Pathol., **52**, 545-552.

Sanbuissho, A., Yoshida, M., Hisada, S., Sagami, F., Kudo, S., Kumazawa, T., Ube, M., Komatsu, S. and Ohno, Y. (2009): Collaborative work on evaluation of ovarian toxicity by repeated-dose and fertility studies in female rats. J. Toxicol. Sci., **34** (Special Issue I), SP1-SP22.

Shirota, M., Watanabe, G., Taya, K. and Sasamoto, S. (1998): Effects of indomethacin on the selective release of follicle-stimulating hormone during the period of ovulation in the rat. J. Vet. Med. Sci., **60**, 1059-65.

Smith, B.J., Plowchalk, D.R., Sipes, I.G. and Mattinson, D.R. (1991): Comparison of random and serial sections in assessment of ovarian toxicity. Reprod. Toxicol., **5**, 379-383.

Stouffer, R.L. (2006): Structure, function, and regulation of the corpus luteum. In the Physiology of Reproduction, Third Edition (Knobil, E., Neill, J.D. eds.), pp.475-526. Raven Press Ltd., New York.

Tamura, T., Yokoi, R., Okuhara, Y., Harada, C., Terashima, Y., Hayashi, M., Nagasawa, T., Onozato, T., Kobayashi, K., Kuroda, J. and Kusama, H. (2009): Collaborative work to evaluate ovarian toxicity 2) Two- or four-week repeated dose studies and fertility study of mifepristone in female rats. J. Toxicol. Sci., **34** (Special Issue I), SP31-SP42.

The ICH Steering Committee to the regulatory authorities of the three ICH regions (the European Union, Japan and USA) (2008): Guidance on nonclinical safety studies for the conduct of human clinical trials and marketing authorization for pharmaceuticals. M3(R2). http://www.pmda.go.jp/ich/m/Step3_m3(r2)_08 _07_14_e.pdf

Tsubota, K., Kushima, K., Yamauchi, K., Matsuo, S., Saegusa, T., Ito, S., Fujiwara, M., Matsumoto, M., Nakatsuji, S., Seki, J. and Oishi, Y. (2009): Collaborative work on evaluation of ovarian toxicity 12) Effects of 2- or 4-week repeated dose studies and fertility study of indomethacin in female rats. J. Toxicol. Sci., **34** (Special Issue I), SP129-SP136.

U.S. Environmental Protection Agency (1998): Health Effects Test Guidelines, OPPTS 870.3800, Reproduction and Fertility Effects. EPA 712-C-98-239. U.S. Environmental Protection Agency, Office of Prevention, Pesticides and Toxic Substances, Washington, DC.

U.S. Food and Drug Administration (2000): Redbook 2000. Toxicological Principles for the Safety Assessment for Food Ingredients. IV.C.9.a. Guidelines for Reproductive Studies. U.S. Food and Drug Administration, Center for Food Safety and Applied Nutrition, Washington, DC.

Watanabe, G., Taya, K. and Sasamoto, S. (1990): Dynamics of ovarian inhibin secretion during the oestrous cycle of the rat. J. Endocrinol., **126**, 151-157.

Westwood, F.R. (2008): The female rat reproductive cycle: A practical histological guide to staging. Toxicol. Pathol., **36**, 375-384.

Yuan, Y.D. and Foley, G.L. (2002): Female Reproductive System. In Handbook of Toxicologic Pathology. Second Edition (Haschek, W.M., Rousseaux, C.G., Walling, M.A. eds.), pp.847-894. Academic Press, San-Diego.

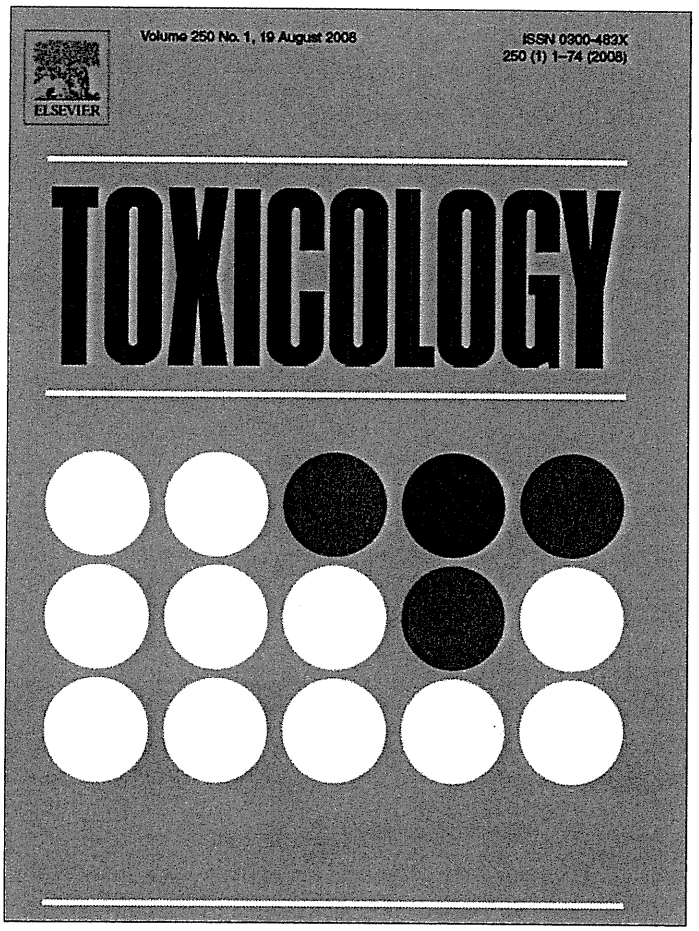

Toxicology 250 (2008) 15–26

Contents lists available at ScienceDirect

Toxicology

journal homepage: www.elsevier.com/locate/toxicol

A toxicogenomics approach for early assessment of potential non-genotoxic hepatocarcinogenicity of chemicals in rats

Takeki Uehara[a], Mitsuhiro Hirode[a], Atsushi Ono[a], Naoki Kiyosawa[a], Ko Omura[a], Toshinobu Shimizu[a], Yumiko Mizukawa[a,b], Toshikazu Miyagishima[a], Taku Nagao[a,c], Tetsuro Urushidani[a,b,*]

[a] Toxicogenomics Project, National Institute of Biomedical Innovation, 7-6-8 Asagi, Ibaraki, Osaka 567-0085, Japan
[b] Department of Pathophysiology, Faculty of Pharmaceutical Sciences, Doshisha Women's College of Liberal Arts, Kodo, Kyotanabe, Kyoto 610-0395, Japan
[c] National Institute of Health Sciences, 1-18-1 Kamiyoga, Setagaya-Ku, Tokyo 158-8501, Japan

ARTICLE INFO

Article history:
Received 14 March 2008
Received in revised form 15 May 2008
Accepted 20 May 2008
Available online 29 May 2008

Keywords:
Toxicogenomics
Rat
Liver
Hepatocarcinogenesis
Non-genotoxic

ABSTRACT

For assessing carcinogenicity in animals, it is difficult and costly, an alternative strategy has been desired. We explored the possibility of applying a toxicogenomics approach by using comprehensive gene expression data in rat liver treated with various compounds. As prototypic non-genotoxic hepatocarcinogens, thioacetamide (TAA) and methapyrilene (MP) were selected and 349 commonly changed genes were extracted by statistical analysis. Taking both compounds as positive with six compounds, acetaminophen, aspirin, phenylbutazone, rifampicin, alpha-naphthylisothiocyanate, and amiodarone as negative, prediction analysis of microarray (PAM) was performed. By training and 10-fold cross validation, a classifier containing 112 probe sets that gave an overall success rate of 95% was obtained. The validity of the present discriminator was checked for 30 chemicals. The PAM score showed characteristic time-dependent increases by treatment with several non-genotoxic hepatocarcinogens, including TAA, MP, coumarin, ethionine and WY-14643, while almost all of the non-carcinogenic samples were correctly predicted. Measurement of hepatic glutathione content suggested that MP and TAA cause glutathione depletion followed by a protective increase, but the protective response is exhausted during repeated administration. Therefore, the presently obtained PAM classifier could predict potential non-genotoxic hepatocarcinogenesis within 24 h after single dose and the inevitable pseudo-positives could be eliminated by checking data of repeated administrations up to 28 days. Tests for carcinogenicity using rats takes at least 2 years, while the present work suggests the possibility of lowering the time to 28 days with high precision, at least for a category of non-genotoxic hepatocarcinogens causing oxidative stress.

1. Introduction

Chemical carcinogenesis is a multistage process, *i.e.*, initiation, promotion and progression (Dragan et al., 1993; Miller and Miller, 1981; Scott et al., 1984). Based on this mechanism of action, chemical carcinogens are classified as genotoxic (mutagenic) and non-genotoxic (non-mutagenic) agents (Hayashi, 1992; Melnick et al., 1996). Genotoxic agents covalently react with DNA to form DNA adducts within the cells of the target organ, contributing to the initiation process. Such chemicals could be assessed by several short-term *in vitro* and *in vivo* assays that measure DNA damage, mutagenic effects, and chromosomal aberrations (Weisburger and Williams, 2000). In the case of non-genotoxic agents, the mechanism is much more complicated. Non-genotoxic carcinogens lack chemical reactivity with DNA and hence do not form DNA adducts, but rather induce effects that indirectly lead to neoplastic transformation or enhance the development of tumors from pre-initiated cells. Although the mechanism of action of such non-genotoxic carcinogens is not fully understood, several possibilities have been postulated in liver, such as oxidative stress, modulation of metabolizing enzymes, induction of peroxisome proliferation, alteration of intercellular communication, and disruption of the balance between proliferation and apoptosis (Butterworth and Bogdanffy, 1999; Cohen and Ellwein, 1990; Klaunig et al., 1998; Klaunig and Kamendulis, 2004; Nguyen-Ba and Vasseur, 1999; Silva Lima and Van der Laan, 2000; Williams et al., 1996). Even more complicated is the fact that many non-genotoxic carcinogens frequently cause several of these effects at once. The effects of non-genotoxic

* Corresponding author at: Department of Pathophysiology, Faculty of Pharmaceutical Sciences, Doshisha Women's College of Liberal Arts, Kodo, Kyotanabe, Kyoto 610-0395, Japan. Tel.: +81 72 641 9826; fax: +81 72 641 9850.
E-mail address: turushid@dwc.doshisha.ac.jp (T. Urushidani).

0300-483X/$ – see front matter © 2008 Elsevier Ireland Ltd. All rights reserved.
doi:10.1016/j.tox.2008.05.013

carcinogens in rodents are only manifested after *in vivo* exposure at high dosage levels over long periods (*e.g.*, 2-year rodent carcinogenicity assays). Consequently, the current strategy for evaluating non-genotoxic carcinogens is not satisfactory because the test is time consuming and expensive, and it requires the use of many animals and large amounts of chemicals.

The present report is focused on the application of toxicogenomics for early assessment of potential non-genotoxic hepatocarcinogenicity of chemicals. Non-genotoxic hepatocarcinogenesis has been studied extensively, and postulated to act via a number of mechanisms: oxidative stress, increased mitogenesis, decreased apoptosis, interference with gap junction intercellular communication, and interference with tubulin polymerization (Combes, 2000; Klaunig et al., 1998). Several recent publications have described applications of microarrays and expression profiling for non-genotoxic carcinogenesis in liver (Ellinger-Ziegelbauer et al., 2005, 2008; Fielden et al., 2007; Nie et al., 2006). They attempted to extract common gene sets coordinately deregulated by several different classes of genotoxic and/or non-genotoxic hepatocarcinogenesis. It was then revealed that the modulation of extracted genes was dependent upon the class of the carcinogenesis. This strongly suggests that mechanism-based strategy should be employed in order to obtain useful biomarker gene sets for carcinogenesis. The specific aim of the present study was to develop identifiers for early assessment of non-genotoxic hepatocarcinogenicity in specific class of chemical based on gene expression profiles in reference to our large-scale database named as TG-GATEs (genomics assisted toxicity evaluation system developed by Toxicogenomics Project, Japan) (Urushidani, 2007). Our strategy was to focus on common gene expression changes in livers treated with two well-known oxidative stressors, methapyrilene (MP) (Lijinsky et al., 1980; National Toxicology Program, 2000; Ohshima et al., 1984; Ratra et al., 1998) and thioacetamide (TAA) (Becker, 1983; Diez-Fernandez et al., 1998; Duivenvoorden and Maier, 1994; Ohtsuka et al., 1998; Sanz et al., 1995) to identify a characteristic set of genes reflecting the early stage of oxidative stress-mediated non-genotoxic hepatocarcinogenesis.

2. Materials and methods

2.1. Animals and experimental design

Five-week-old male Sprague–Dawley rats were obtained from Charles River Japan, Inc. (Kanagawa, Japan). After a 7-day quarantine and acclimatization period, the animals (6-week old) were assigned to dosage groups (five rats per group) using a computerized stratified random grouping method based on individual body weight. The animals were individually housed in stainless-steel cages in an animal room that was lighted for 12 h (7:00–19:00) daily, ventilated with an air-exchange rate of 15 times per hour, and maintained at 21–25 °C with a relative humidity of 40–70%. Each animal was allowed free access to water and pellet diet (CRF-1, sterilized by radiation, Oriental Yeast Co., Ltd., Tokyo, Japan).

Table 1 lists the overview of the compounds used in this study. A total of 30 compounds (10 non-genotoxic hepatocarcinogens and 20 non-hepatocarcinogens) were available in the database when the present analysis was performed. They were subdivided in a training set, consisting of 2 non-genotoxic carcinogens (positive training set) and 6 non-hepatocarcinogens (negative training set) with the test set for additional validation consisting of 8 non-genotoxic carcinogens and 14 non-hepatocarcinogens.

According to the standard protocol in our project (Takashima et al., 2006), five rats per group were orally administered at three doses with these compounds suspended or dissolved either in 0.5% methylcellulose (MC) solution or corn oil according to their dispersibility. Traditionally, carcinogenicity studies for chemical agents have relied upon the maximally tolerated dose (MTD) as the standard method for high dose selection. In the present study, the MTD was chosen based on data derived from preliminary toxicity studies of 7 days duration.

For single-dose studies, rats were sacrificed at 3, 6, 9 and 24 h after dosing (3H, 6H, 9H and 24H, respectively). For repeated dose studies, the animals were treated daily for 3, 7, 14 and 28 days, and sacrificed 24 h after the last dosing [day 4 (4D), 8 (8D), 15 (15D) and 29 (29D), respectively]. The animals were euthanized by exsanguination from the abdominal aorta under ether anesthesia, and the liver samples were obtained from the left lateral lobe of the liver in each animal immediately after sacrifice for examination.

The experimental protocols were reviewed and approved by the Ethics Review Committee for Animal Experimentation of National Institute of Health Sciences.

2.2. Histopathology of livers treated with MP or TAA

For light microscopical examination, the liver sample of each animal was fixed in 10% neutral buffered formalin, dehydrated in alcohol and embedded in paraffin. Paraffin sections were prepared and stained by a routine method with hematoxylin and eosin (H&E).

2.3. Microarray analysis

An aliquot of the sample (about 30 mg) for microarray analysis was obtained from the left lateral lobe of the liver in each animal immediately after sacrifice, kept in RNAlater® (Ambion, Austin, TX, USA) overnight at 4 °C, and then frozen at −80 °C until use. Liver samples were homogenized with the buffer RLT supplied in RNeasy Mini Kit (Qiagen, Valencia, CA, USA), and total RNA was isolated according to the manufacturer's instructions. Microarray analysis was conducted on three out of five samples for each group by using GeneChip® RAE230A probe arrays (Affymetrix, Santa Clara, CA, USA). The procedure was basically conducted according to the manufacture's instructions as previously reported (Uehara et al., 2008a,b). Microarray Analysis Suite 5.0 (MAS; Affymetrix) was used to quantify microarray signals and the intensities were normalized for each chip by setting the mean intensity to 500 (per chip normalization).

2.4. Selection of persistently up/down-regulated genes in common with MP and TAA

By using statistical and clustering tools, persistently up/down-regulated genes in common with MP and TAA throughout the study periods were extracted. First, data were imported into GeneSpring 6.0 software (Silicon Genetics, Redwood City, CA), and comparisons among time-matched groups from each study of MP and TAA were performed using one-way analysis of variance (ANOVA) with Tukey's multiple comparison test for post hoc comparisons when significance was determined by ANOVA with a false discovery rate ($p < 0.05$). Probe sets exhibiting significant changes in expression by Tukey's multiple comparison test in both high- and middle-dose groups for one or more time points in each study were selected. In the next step, significant selected probe sets (452 probe sets) were divided into subsets with distinct expression profiles by K-means clustering using Tigr Mev 3.1 software (http://www.tm4.org/mev.html) (current metric: Euclidean distance; divided into nine clusters) based on logarithm (log 2) of the ratio to control for individual gene expression. Genes not categorized in the clusters showing clear time- and dose-independent expression pattern were excluded from further analysis. Finally, a subset of 349 probe sets containing 276 up-regulated and 73 down-regulated probe sets was selected for common intersection to single and repeated studies of MP and TAA (for more information, see supplemental figures).

2.5. Class discrimination by prediction analysis of microarray (PAM)

Prediction of potential carcinogenesis was performed by an approach using PAM for R package (http://www-stat.stanford.edu/~tibs/PAM). PAM makes sample classification using the nearest shrunken centroid method with an automated gene selection step integrated into the algorithm (Tibshirani et al., 2002). It employs a parameter threshold Δ to select genes for class discrimination. PAM training is performed by comparing 2 positive compounds as non-genotoxic carcinogenesis (MP and TAA, high dose group only) with 6 negative compounds, *i.e.*, APAP (Iida et al., 2005; National Toxicology Program, 1993), ASA (Giri, 1993), PhB (Meakawa et al., 1987; National Toxicology Program, 1990), RIF (Sodhi et al., 1997), ANIT (Jean and Roth, 1995; Leonard et al., 1981) and AM (Agoston et al., 2003; Delaney et al., 2004) for the ratio of expression levels of the selected 349 probe sets at various time points (a total of 64 training samples).

Ten-fold cross validation was performed to find out the optimal classifier performance, which minimized classification errors for training sets. During the validation, a threshold Δ was varied in search of the optimal classifier performance. The Δ value that settled at the lowest classification error with the fewest genes was favored as the optimal. For validation of the classifier, the optimized threshold value obtained from training was subsequently used for prediction of potential carcinogenicity for the total of 30 compounds, including training sets. PAM prediction results were expressed as a logarithm transformed score (PAM prediction score) of the ratio of positive class probability relative to negative class probability associated with the classification of each sample, *i.e.*,

$$\text{PAM prediction score} = \log_{10} \frac{\text{class probability : positive}}{\text{class probability : negative}}$$

Table 1
Overview of the compounds used for prediction analysis of microarrays training and/or test

Compound	Abbreviation	CAS-number	Mode of action	Supplier	Vehicle	Dose (mg/kg)	PAM training/test
Non-genotoxic hepatocarcinogens[a,b]							
Methapyrilene	MP	135-23-9	Oxidative stress induction	Sigma	0.5%MC	10, 30, 100	Positive training/test set
Thioacetamide	TAA	62-55-5	Oxidative stress induction	Sigma	0.5%MC	4.5, 15, 45	Positive training/test set
Coumarin	CMA	91-64-5	Oxidative stress induction	Tokyo Chemical Industry	Corn oil	150	Test set
Ethionine	ET	67-21-0	Oxidative stress induction	Tokyo Chemical Industry	0.5%MC	250	Test set
Carbon tetrachloride	CCL4	56-23-5	Oxidative stress induction	Wako Pure Chemical Industries	Corn oil	300	Test set
Phenobarbital	PB	57-30-7	Hepatic enzyme induction	Sigma	0.5%MC	100	Test set
Hexachlorobenzene	HCB	118-74-1	Hepatic enzyme induction	Tokyo Chemical Industry	Corn oil	300	Test set
Clofibrate	CFB	637-07-0	Peroxisome proliferation	Wako Pure Chemical Industries	Corn oil	300	Test set
Gemfibrozil	GFZ	25812-30-0	Peroxisome proliferation	Sigma	Corn oil	300	Test set
Wy-14,643	WY	50892-23-4	Peroxisome proliferation	Tokyo Chemical Industry	Corn oil	100	Test set
Non-hepatocarcinogens[a,b]							
Acetaminophen	APAP	103-90-2	–	Sigma	0.5%MC	600	Negative training set
Aspirin	ASA	50-78-2	–	Wako Pure Chemical Industries	0.5%MC	450	Negative training set
Phenylbutazone	PhB	50-33-9	–	Sigma	0.5%MC	200	Negative training set
Rifampicin	RIF	13292-46-1	–	Wako Pure Chemical Industries	0.5%MC	200	Negative training set
Alpha-naphthylisothiocyanate	ANIT	551-06-4	–	Tokyo Chemical Industry	Corn oil	15	Negative training set
Amiodarone hydrochloride	AM	1951-25-3	–	Sigma	0.5%MC	200	Negative training set
Allopurinol	APL	315-30-0	–	Sigma	0.5%MC	150	Negative test set
Allyl alcohol	AA	107-18-6	–	Tokyo Chemical Industry	Corn oil	30	Negative test set
Benzbromarone	BBr	3562-84-3	–	Sigma	0.5%MC	200	Negative test set
Bromobenzene	BBZ	108-86-1	–	Tokyo Chemical Industry	Corn oil	300	Negative test set
Carbamazepine	CBZ	298-46-4	–	Sigma	0.5%MC	300	Negative test set
Chlorpromazine	CPZ	69-09-0	–	Wako Pure Chemical Industries	0.5%MC	45	Negative test set
Diclofenac sodium	DFNa	15307-79-6	–	Cayman Chemical Company	0.5%MC	10	Negative test set
Diazepam	DZP	439-14-5	–	Wako Pure Chemical Industries	0.5%MC	250	Negative test set
Isoniazid	INAH	54-85-3	–	Sigma	0.5%MC	200	Negative test set
Nitrofurantoin	NFT	67-20-9	–	ICN Biomedicals	0.5%MC	100	Negative test set
Phenytoin	PHE	57-41-0	–	Tokyo Chemical Industry	0.5%MC	600	Negative test set
Propylthiouracil	PTU	51-52-5	–	Tokyo Chemical Industry	0.5%MC	100	Negative test set
Sulfasalazine	SS	599-79-1	–	Sigma	0.5%MC	1000	Negative test set
Valproate sodium	VPA	1069-66-5	–	Sigma	0.5%MC	450	Negative test set

[a] Genotoxicity is based on *in vitro* genotoxicity tests (Salmonella and mammalian gene mutation tests) as reviewed in NTP (http://ntp-server.niehs.nih.gov/), IARC (http://monographs.iarc.fr.) and several published papers.
[b] Carcinogenicity is based on reviews by NTP (http://ntp-server.niehs.nih.gov/), IARC (http://monographs.iarc.fr.) and several published papers.

2.6. Gene ontology (GO) analysis of PAM classifier

The identified probe sets were subjected to GO analysis by DAVID (database for annotation, visualization, and integrated discovery; http://apps1.niaid.nih.gov/david/) using Fisher's exact test. Level 3 analysis was adopted.

2.7. Measurement for hepatic total glutathione contents

Hepatic total glutathione was measured in the liver of rats receiving a high dose of MP, TAA or BBZ, and their corresponding controls. Measurements were performed for three rats (gene expression was measured) per group using Glutathione Quantification Kit (Dojindo Mol. Tech, Inc., Kumamoto, Japan). In brief, the liver tissue was homogenized in 5% 5-sulfosalicylic acid and the particulate cellular debris was removed by centrifugation ($8000 \times g$) for 10 min. The internal standards consist of serial dilutions of glutathione (1000, 750, 500, 250, 100, 50 and 0 μM). The change in absorbance at 405 nm was measured and total glutathione was calculated according to the glutathione standard curve. The results were analyzed with the use of an unpaired two-tailed Student's *t*-test or Welch's *t*-test as appropriate, and a *p*-value of <0.05 was considered statistically significant.

3. Results

3.1. Histopathology

Except for the death of one animal in the high dose group of MP on 20D, there were no other deaths in these studies of MP and TAA.

MP- or TAA-treated rats revealed typical liver damage throughout the study periods. Although the extent of the liver damage differed slightly among the animals, a similar pattern was obtained for those in the same dose group.

At high dosage of MP in the single dose study, periportal hepatocytes exhibited hypertrophy characterized by granular eosinophilic cytoplasm and enlarged nuclei with variable anisonucleosis at each time point. More striking abnormalities include mononuclear cell infiltration and hepatocellular single cell necrosis containing shrunken cells with pyknotic nuclei randomly scattered throughout the periportal region of the hepatic lobule. Associated with these lesions, increased numbers of hepatocellular mitotic figures and bile duct hyperplasia were present at each time point in the repeated dose study. At 29D, hepatocellular hyperplasia became evident, and some affected portal regions contained an increased number of oval cells arranged in clusters without a distinct lumen (Fig. 1a). In addition, for the same dose group, a pre-neoplastic altered hepatocellular focus was also observed (Fig. 1b). Middle-dose MP treatment resulted in minimal hepatocellular hypertrophy, single cell necrosis of hepatocytes, and mononuclear cell infiltration in the periportal region at 15D and 29D. Moreover, no significant histopathological alterations were observed at early time points except hepatocellular hypertrophy. In the low-dose MP-treated groups, no significant changes were observed throughout the study periods except for minimal hypertrophy of hepatocytes, observed in one animal each at 8D and 29D.

At high- and middle-dose of TAA, centrilobular hepatocytes exhibited hypertrophy with large, atypical nuclei in single and repeated dose studies (Fig. 1c). Moreover inflammatory cell infiltration and hepatocellular single cell necrosis were also observed at the centrilobular region. The degree of these lesions increased in a dose and time-dependent manner. At 15D and 29D, bile duct hyperplasia and oval cell proliferation at the periportal region became evident, and a pre-neoplastic altered hepatocellular focus was also observed (Fig. 1d). No significant histopathological alterations were observed in the low-dose groups throughout the study periods except degeneration of hepatocytes with granular and eosinophilic cytoplasm, observed in two animals at 29D.

3.2. Class discrimination by PAM in the training set

PAM training was performed using the training set to identify a minimal subset of genes expected to best characterize the early stage of non-genotoxic hepatocarcinogenesis-specific responses. Fig. 2 shows the training and cross-validation errors for different threshold values. Both the training and cross-validated errors were minimized near the threshold = 4.00, where 112 genes were selected. At this threshold, both classes of the training samples were clearly separated based on the expression pattern of these 112 genes with an overall success rate of 95%. Namely, 13 of the 16 positive sets (81%) and all of the negative sets (100%) were correctly classified (Fig. 3a). However, three positive sets (MP-3H, -4D and TAA-3H) were classified as negative, together with all of the negative sets (Fig. 3b).

The list of the genes involved in the PAM classifier is shown in Table 2 (for more information, see supplemental data). Genes were sorted according to the best prediction between the two classes. The top three important discriminators identified by PAM were "nuclear RNA helicase, DECD variant of DEAD box family (Ddx39)", "interferon-related developmental regulator 1 (Ifrd1)", and "mdm2, transformed mouse 3T3 cell double minute 2 (Mdm2)", which were highly up-regulated by MP and TAA. In the extracted 112 probe sets, 111 were prominently up-regulated in the positive training set and the remaining 1 gene (cytochrome P450 4F4) was down-regulated. Based on gene ontology, the contents of genes related to cellular metabolism including several anti-oxidative metabolism, cell proliferation, cell cycle, response to DNA damage stimulus were significantly high (Table 3). These features might reflect the cellular changes related to sustained oxidative stress in association with non-genotoxic hepatocarcinogenesis by MP and TAA.

3.3. Validation of usefulness of the PAM classifier

The 112-gene classifier generated on the training set was next applied to class discrimination for the 30 total compounds as a validation test. The classifier predicted the following samples as positive: high dose MP-6H, 9H, 24H, 8D, 15D and 29D; middle-dose TAA-29D; high dose TAA-6H, 9H, 24H, 4D, 8D, 15D and 29D; CMA-3H, 6H and 9H; ET-24H, 4D, 8D, 15D and 29D; WY-15D and 29D; BBZ-24H. All of other samples (including enzyme inducers, PB and HCB; peroxisome proliferators other than WY, such as CFB and GFZ; and other compounds) were predicted as negative.

In the present study, these prediction results were visualized as a numerical score reflecting the probabilities of class discrimination between the two classes, namely the PAM prediction score. The PAM score showed characteristic time-dependent changes by treatment with several non-genotoxic hepatocarcinogens. In the MP- or TAA-treated group, the score increased dose-dependently with a peak value at 6H for MP, 9H and 24H for TAA after single dosing, and then it markedly increased with repeated administrations (Fig. 4b, c, e, f). CMA, ET or WY treatment also resulted in an increase in the score with a peak value at 6H for CMA, 24H for ET and WY, and also showed an increase or tendency to increase with repeated dosing (Fig. 4g, h, j). Although all of the CCL4-treated groups were predicted as negative, the score showed a tendency to increase with repeated dosing (Fig. 4i). On the other hand, all of the low dose MP- or TAA-treated groups were predicted as negative without any tendency to increase in the score with repeated dosing (Fig. 4a and d). As for the enzyme inducers with carcinogenic activity, PB and HCB (Fig. 4l and m), and peroxisome proliferators other than WY, *i.e.*, CFB (Fig. 4n) and GFZ (within Fig. 4r), showed negative scores throughout the time points. Of the non-carcinogenic samples, BBZ showed a transient increase in the score at 24H but returned to negative during repeated dosing (Fig. 4k). Other non-carcinogenic

Table 2
The list of the genes involved in the PAM classifier

Probe ID	Accession number	Gene title	Gene symbol
1387048_at	NM_053563	DEAD (Asp-Glu-Ala-Asp) box polypeptide 39	Ddx39
1367795_at	NM_019242	Interferon-related developmental regulator 1	Ifrd1
1384427_at	XM_001080981	Transformed mouse 3T3 cell double minute 2 homolog (mouse) (predicted)	Mdm2_predicted
1388986_at	–	EST	–
1369921_at	NM_020540	Glutathione *S*-transferase M4	Gstm4
1368072_at	NM_019290	B-cell translocation gene 3	Btg3
1387060_at	NM_031642	Kruppel-like factor 6	Klf6
1376098_a_at	XM_001069724	Myosin IG	Myo1g
1368173_at	NM_021754	Nucleolar protein 5	Nol5
1373200_at	XM_001063564	Eukaryotic translation elongation factor 1 epsilon 1 (predicted)	Eef1e1_predicted
1388560_at	NM_001008771	WD repeat domain 77	Wdr77
1374945_at	NM_001007706	GCD14/PCMT domain containing protein RGD1359191	RGD1359191
1376737_at	XM_001073157	EST	LOC686259
1388397_at	NM_001008721	EBNA1 binding protein 2	Ebna1bp2
1371785_at	NM_181086	Tumor necrosis factor receptor superfamily, member 12a	Tnfrsf12a
1375895_at	–	EST	–
1367764_at	NM_012923	Cyclin G1	Ccng1
1388674_at	NM_080782	Cyclin-dependent kinase inhibitor 1A	Cdkn1a
1373499_at	NR_002704	Growth arrest specific 5	Gas5
1386897_at	NM_024363	Heterogeneous nuclear ribonucleoproteins methyltransferase-like 2 (*S. cerevisiae*)	Hrmt1l2
1372211_at	NM_145673	v-maf musculoaponeurotic fibrosarcoma oncogene family, protein K (avian)	Mafk
1386995_at	NM_017259	B-cell translocation gene 2, anti-proliferative	Btg2
1372510_at	NM_001047858	Sulfiredoxin 1 homolog (*S. cerevisiae*)	Srxn1
1388900_at	XM_001076548	RGD1566118 (predicted)	RGD1566118_predicted
1370583_s_at	NM_012623	ATP-binding cassette, sub-family B (MDR/TAP), member 1A/1B	Abcb1a/Abcb1b
1398756_at	NM_012992	Nucleophosmin 1	Npm1
1375224_at	NM_001012206	Pleckstrin homology-like domain, family A, member 3	Phlda3
1388155_at	NM_053976	Keratin complex 1, acidic, gene 18	Krt1-18
1368032_at	NM_022869	Nucleolar and coiled-body phosphoprotein 1	Nolc1
1388629_at	NM_199099	Inosine 5-monophosphate dehydrogenase 2	Impdh2
1371936_at	NM_199372	Eukaryotic translation initiation factor 4A1	Eif4a1
1377387_a_at	–	EST	–
1374326_at	NM_001011980	Peter pan homolog (Drosophila)	Ppan
1367617_at	NM_012495	Aldolase A	Aldoa
1376001_at	XM_001065234	Polymerase (RNA) I associated factor 1 (predicted)	Praf1_predicted
1398832_at	NM_012749	Nucleolin	Ncl
1368121_at	NM_013215	Aldo–keto reductase family 7, member A3 (aflatoxin aldehyde reductase)	Akr7a3
1370174_at	NM_133546	Myeloid differentiation primary response gene 116	Myd116
1398771_at	NM_019283	Solute carrier family 3, member 2	Slc3a2
1389450_at	XM_001071583	EST	LOC360830
1371530_at	NM_199370	Keratin complex 2, basic, gene 8	Krt2-8
1367834_at	NM_053464	Spermidine synthase	Srm
1387282_at	NM_053612	Heat shock 22 kDa protein 8	Hspb8
1372043_at	XM_001071573	EST	RGD1311709_predicted
1372150_at	NM_001034146	Ubiquitin-specific protease 10	Usp10
1389569_at	NM_001029915	Brix domain containing 2	Bxdc2
1371498_at	NM_001037348	JTV1	MGC125271
1389815_at	NM_172045	Protein phosphatase 1, regulatory (inhibitor) subunit 14B	Ppp1r14b
1370314_at	NM_031148	Solute carrier family 20, member 1	Slc20a1
1372218_at	NM_199410	WD repeat domain 12	Wdr12
1372354_at	–	EST	–
1367654_at	NM_031819	Fat tumor suppressor homolog (Drosophila)	Fath
1388107_at	NM_144746	Protein phosphatase 2, regulatory subunit B, delta isoform	Ppp2r2d
1372028_at	NM_001047095	EST	RGD1305727_predicted
1373767_at	NM_001008363	Zinc finger, AN1-type domain 2A	Zfand2a
1390579_at	XM_001073162	EST	RGD1305222_predicted
1388588_at	NM_001015013	Mammary tumor virus receptor 2	Mtvr2
1370309_a_at	NM_031330	Heterogeneous nuclear ribonucleoprotein A/B	Hnrpab
1367732_at	NM_030987	Guanine nucleotide binding protein, beta 1	Gnb1
1399158_a_at	NM_012992	Nucleophosmin 1	Npm1
1389577_at	NM_001009640	Cirrhosis, autosomal recessive 1A (human)	Cirh1a
1398757_at	NM_012992	Nucleophosmin 1	Npm1
1370947_at	XM_001070821	EST	Rda279
1373677_at	XM_001061829	Solute carrier family 39 (zinc transporter), member 10 (predicted)	Slc39a10_predicted
1388244_s_at	NM_017138	Ribosomal protein SA	Rpsa
1388150_at	NM_053490	Exportin 1, CRM1 homolog (yeast)	Xpo1
1388666_at	NM_001003401	Ectodermal–neural cortex 1	Enc1
1367713_at	NM_019356	Eukaryotic translation initiation factor 2, subunit 1 alpha	Eif2s1
1386910_a_at	NM_024148	Apurinic/apyrimidinic endonuclease 1	Apex1
1372019_at	XM_001062474	EST	RGD1310128_predicted
1373647_at	NM_001009652	Zinc finger protein 622	Zfp622
1387072_at	NM_053794	Protein kinase, lysine deficient 1	Prkwnk1
1388754_at	–	EST	–
1367870_at	NM_032614	Thioredoxin-like 2	Txnl2

Table 2 (*Continued*)

Probe ID	Accession number	Gene title	Gene symbol
1387950_at	NM_138847	Nuclear import 7 homolog (*S. cerevisiae*)	Nip7
1387807_at	NM_031763	Platelet-activating factor acetylhydrolase, isoform Ib, alpha subunit 45 kDa	Pafah1b1
1371378_at	XM_001053247	EST	LOC678808
1371735_at	–	EST	–
1398791_at	NM_031614	Thioredoxin reductase 1	Txnrd1
1386958_at	NM_031614	Thioredoxin reductase 1	Txnrd1
1385616_a_at	XM_001059946	ASF1 anti-silencing function 1 homolog A (*S. cerevisiae*) (predicted)	Asf1a_predicted
1388990_at	NM_139186	Mki67 (FHA domain) interacting nucleolar phosphoprotein	Mki67ip
1388449_at	XM_001071102	Eukaryotic translation elongation factor 1 beta 2 (predicted)	Eef1b2_predicted
1373850_at	NM_001025737	Sphingomyelin phosphodiesterase, acid-like 3B	Smpdl3b
1371539_at	XM_001071992	Nucleolar protein family A, member 2 (predicted)	Nola2_predicted
1387774_at	NM_013011	Tyrosine 3-monooxygenase/tryptophan 5-monooxygenase activation protein, zeta polypeptide	Ywhaz
1371980_at	NM_001034922	ATPase family, AAA domain containing 3A	Atad3a
1373075_at	XM_001061556	EST	RGD1560888_predicted
1367693_at	NM_013052	Tyrosine 3-monooxygenase/tryptophan 5-monooxygenase activation protein, eta polypeptide	Ywhah
1387973_at	NM_173123	Cytochrome P450, family 4, subfamily f, polypeptide 4	Cyp4f4
1390317_at	–	EST	–
1371377_at	NM_001037346	Ribosomal protein S19	Rps19
1373380_at	NM_001010963	Brain zinc finger protein	LOC362154
1367590_at	NM_053439	RAN, member RAS oncogene family	Ran
1370295_at	NM_138548	Expressed in non-metastatic cells 1	Nme1
1374632_at	NM_001012143	Phosphatidylserine receptor	Ptdsr
1388381_at	NM_001013095	Eukaryotic translation initiation factor 3, subunit 4 (delta)	Eif3s4
1370785_s_at	NM_152935	Translocase of outer mitochondrial membrane 20 homolog (yeast)	Tomm20
1398801_at	NM_134415	CDK105 protein	Cdk105
1374764_at	XM_001058941	EST	RGD1305605_predicted
1374793_at	XM_001065786	WD repeat domain 3 (predicted)	Wdr3_predicted
1368106_at	NM_031821	polo-like kinase 2 (Drosophila)	Plk2
1372116_at	XM_001079091	Mitochondrial ribosomal protein S2 (predicted)	Mrps2_predicted
1388507_at	NM_001037352	Integrin beta 4 binding protein	Itgb4bp
1389200_at	NM_182674	Bystin-like	Bysl
1372558_at	XM_001053949	NMDA receptor-regulated gene 1 (predicted)	Narg1_predicted
1371809_at	NM_212534	Mitochondrial ribosomal protein S18B	Mrps18b
1387911_at	NM_138708	RAB geranylgeranyl transferase, b subunit	Rabggtb
1372243_at	XM_001063411	Calcium binding protein 39 (predicted)	Cab39_predicted
1372255_at	XM_001065238	Arginyl-tRNA synthetase (predicted)	Rars_predicted
1370184_at	NM_017147	Cofilin 1, non-muscle	Cfl1
1372461_at	NM_001012504	EST	Set_predicted

compounds including APL, AA, and BBr (Fig. 4o–q), and remaining 16 (Fig. 4r) were correctly predicted as negative.

3.4. Additional biological validation

In order to support the class discrimination results by PAM, hepatic total glutathione was quantified for the following selected samples: high dose MP- and TAA-treated groups, and BBZ-treated groups.

Hepatic glutathione contents transiently reduced with peak values at 3H for MP, 6H for TAA and 9H for BBZ after single dosing, and rapidly recovered 24H after the treatment (Fig. 5). Although hepatic glutathione content was kept at normal or higher in the BBZ-treated group at all time points of repeated dose study, in the MP- and TAA-treated groups it reduced with repeated dosing (Fig. 5). These time course changes of the glutathione contents are clearly correlated with the change of the PAM score.

Of the PPARα agonists, only WY, but not CFB and GFZ, showed positive scores at 15D and 29D. If the PAM classifier detects carcinogenesis via the activation of PPARα and these three agonists stimulated the receptor to the same extent, all of three agonists should have been classified as positive. The dose of each compound had been determined based on a 7-day repeated preliminary study and thus the doses would not be proportional to their potency to the receptor. To assess the biological potency of each agonist *in vivo*, we compared the induction of acyl-coenzyme A oxidase 1, a gene directly regulated by PPARα. As shown in Fig. 6, the dose of WY appeared to be too high, since enzyme induction reached its maximum by the low dose of WY. During repeated administrations, however, the extent of the induction was almost the same as in the high dose of these three agonists. If the positive score of WY was due to its PPARα activation, not only the high dose but also the middle and low dose should be classified as positive. We then performed PAM using the present classifier for the three doses of these three agonists, but no positive scores were obtained other than the high dose of WY at 15D and 29D (data not shown).

4. Discussion

The goal of the present study was to develop a classifier for early assessment of potential non-genotoxic hepatocarcinogenic-

Table 3
GO analysis of the PAM classifier

Term	Count	Percentage	*p*-Value
Cellular metabolism	41	34.75	5.07E–03
Primary metabolism	38	32.20	1.80E–02
Macromolecule metabolism	31	26.27	8.64E–04
Cell organization and biogenesis	22	18.64	3.84E–05
Biosynthesis	14	11.86	8.19E–03
Cellular localization	12	10.17	3.03E–04
Cell proliferation	10	8.47	6.26E–03
Negative regulation of physiological process	10	8.47	1.66E–02
Negative regulation of cellular process	10	8.47	2.75E–02
Protein localization	9	7.63	7.12E–03
Cell cycle	9	7.63	1.10E–02
Cell death	8	6.78	4.27E–02
Cellular morphogenesis	7	5.93	2.60E–02
Response to DNA damage stimulus	5	4.24	2.58E–02
Regulation of response to stimulus	2	1.69	2.33E–02

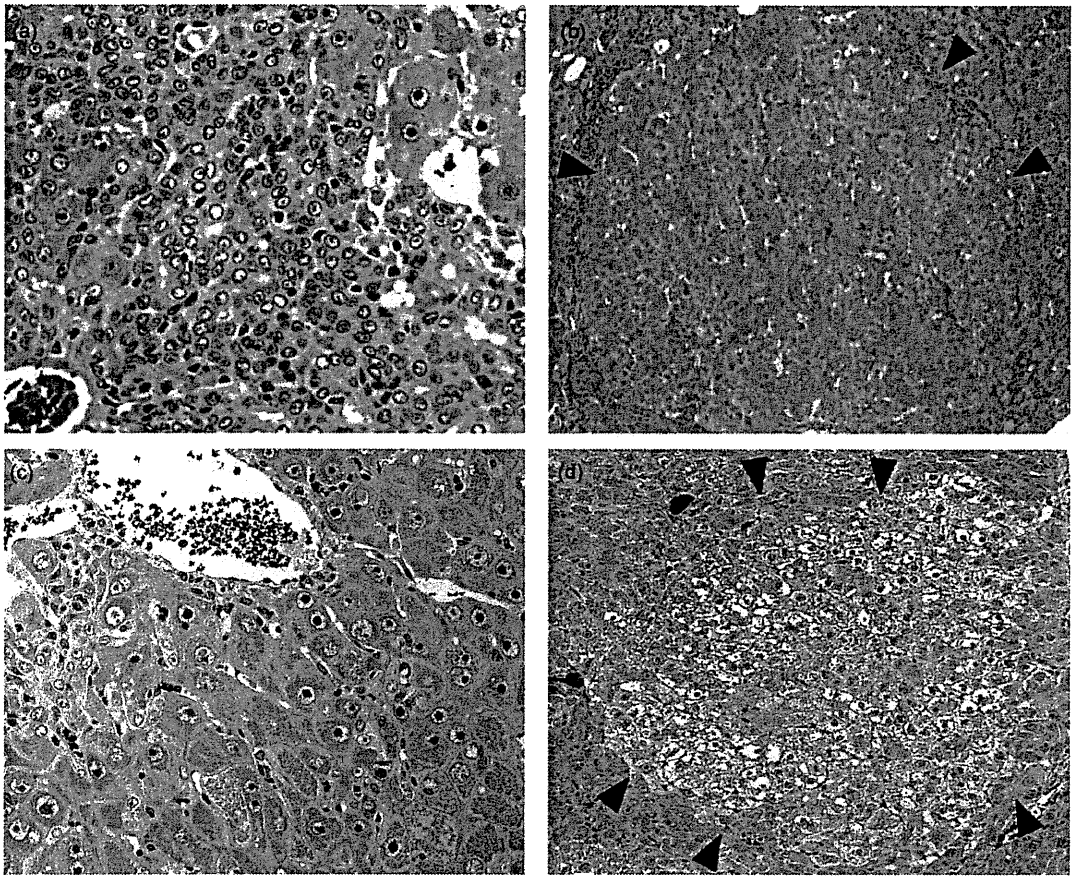

Fig. 1. Histopathology of rat liver treated with MP or TAA for 28 days. Repeated administrations of high dose of MP (100 mg/kg) for 28 days caused hepatocellular hyperplasia and some affected portal regions contained increased numbers of oval cells arranged in clusters without a distinct lumen (a), and in some cases, a pre-neoplastic altered hepatocellular focus was seen (b; arrowheads). In the centrilobular region of rat liver treated with repeated administrations of high dose of TAA (45 mg/kg) for 28 days, hepatocytes exhibited hypertrophy with large, atypical nuclei (c). As in methapyrilene, a pre-neoplastic altered hepatocellular focus was also observed (d; arrowheads).

ity of chemicals based on gene expression changes stored in our database, TG-GATEs. In order to utilize the classifier for practical drug development, we did not attempt to explore an original algorism but to use a well-established one, *i.e.*, PAM in the present case. Our advantage over the previous similar works was the quality of the database, *i.e.*, the quantitative gene expression data obtained in the single platform employing standardized and enriched protocol with three dose levels and eight time points (four for single and four for repeated). The enrichment of time and dose in the data has been shown to be quite powerful in toxicological analysis in various

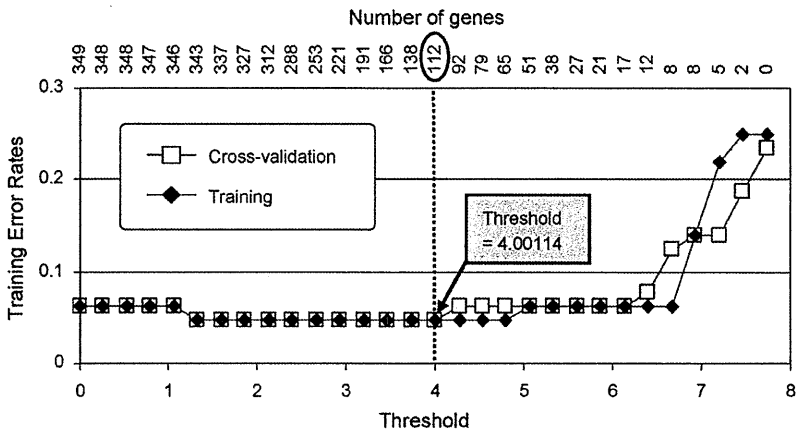

Fig. 2. PAM training and cross validation. PAM training was performed by comparing 2 positive compounds (MP and TAA, high dose group only) with 6 negative compounds (APAP, ASA, PhB, RIF, ANIT and AM) on the ratio of expression levels of the selected 349 probe sets for various time points (total of 64 training samples). Ten-fold cross validation was performed to find out the optimal classifier performance, which minimized classification errors for training sets. Both the training (black symbol) and cross-validated errors (white symbol) were minimized near the threshold = 4.00, where 112 genes (circled) were selected.

(a)

		Prediction results			
		Positive	Negative	Class Error Rate	Overall Error Rate
Training	Positive	13	3	0.19	0.05
	Negative	0	48	0.00	

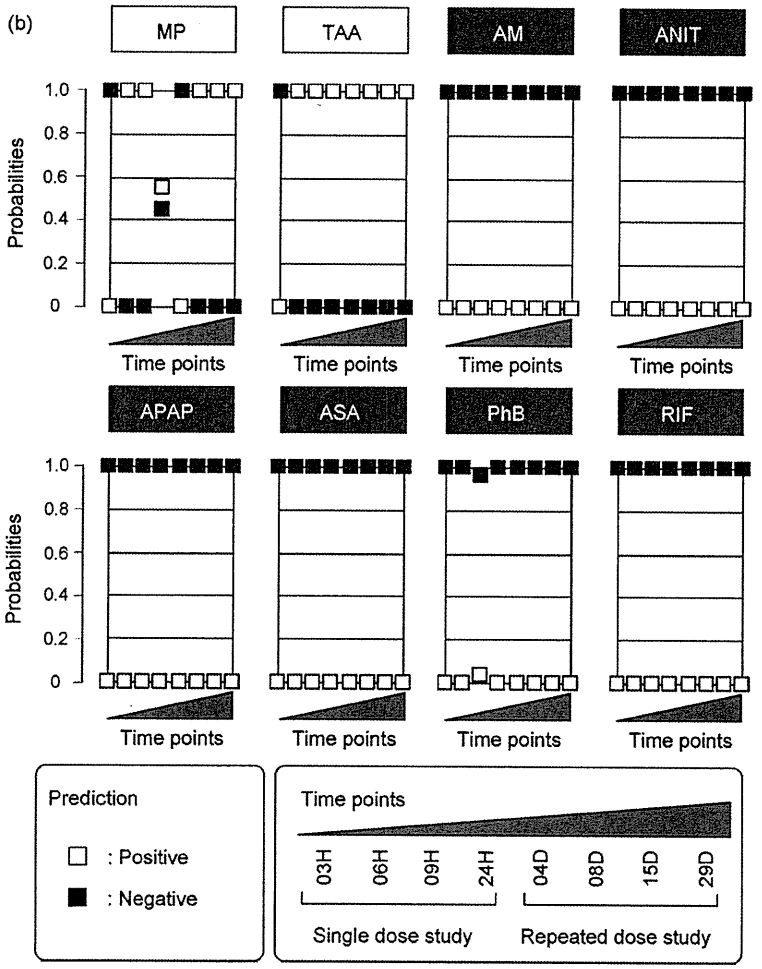

Fig. 3. Class discrimination by PAM. PAM prediction results for the condition determined in Fig. 2 are shown. (a) Prediction results of the training sets (13 positives and 48 negatives) are shown. Note that the overall success rate was 95%, *i.e.*, 13 of the 16 positive sets (81%) and all of the negative sets (100%) were correctly classified. (b) Prediction result of individual sample. For each chemical, the samples are aligned with time as shown on the bottom. The samples predicted as positive are depicted with white and negative with black. Note that two out of three errors occurred at 3 h after single dosing.

ways (Urushidani, 2007). In the present study, genes showing clear dose- and time-dependent changes were successfully extracted by K-means clustering, and we could detect the changes of the score transient after single administration which then turned to be sustained after repeated administration. These also helped us consider the toxicological mechanism.

After PAM training, we produced a discriminator consisting of 112 of the mobilized probe sets that could discriminate between both classes with a high probability, >95%. In the training procedure, MP-3H, 4D, and TAA-3H were judged as false negatives. However, these results were considered to be reasonable because 3H of both compounds was too early for development of hepatotoxicity and 4D of MP treatment was the period when homeostatic recovery of the hepatic glutathione contents occurred.

In the present experiments, MP and TAA showed similar early morphological changes in rat liver, characterized as hepatocellular single cell necrosis with inflammatory response and hypertrophy with granular eosinophilic changes. This was confirmed by electron microscopy as proliferation and swelling of mitochondria (unpublished observations). In addition, hepatocellular altered foci were observed at 15D and/or 29D in the MP and TAA-treated groups. It is well known that this type of lesion is a pre-neoplastic transformation of the cells and is induced in the early stage of non-genotoxic hepatocarcinogenesis in the liver (Bannasch, 1976; Fischer et al., 1983). Therefore, early gene expression profiling in liver treated with these two compounds is considered to be closely related to future carcinogenesis.

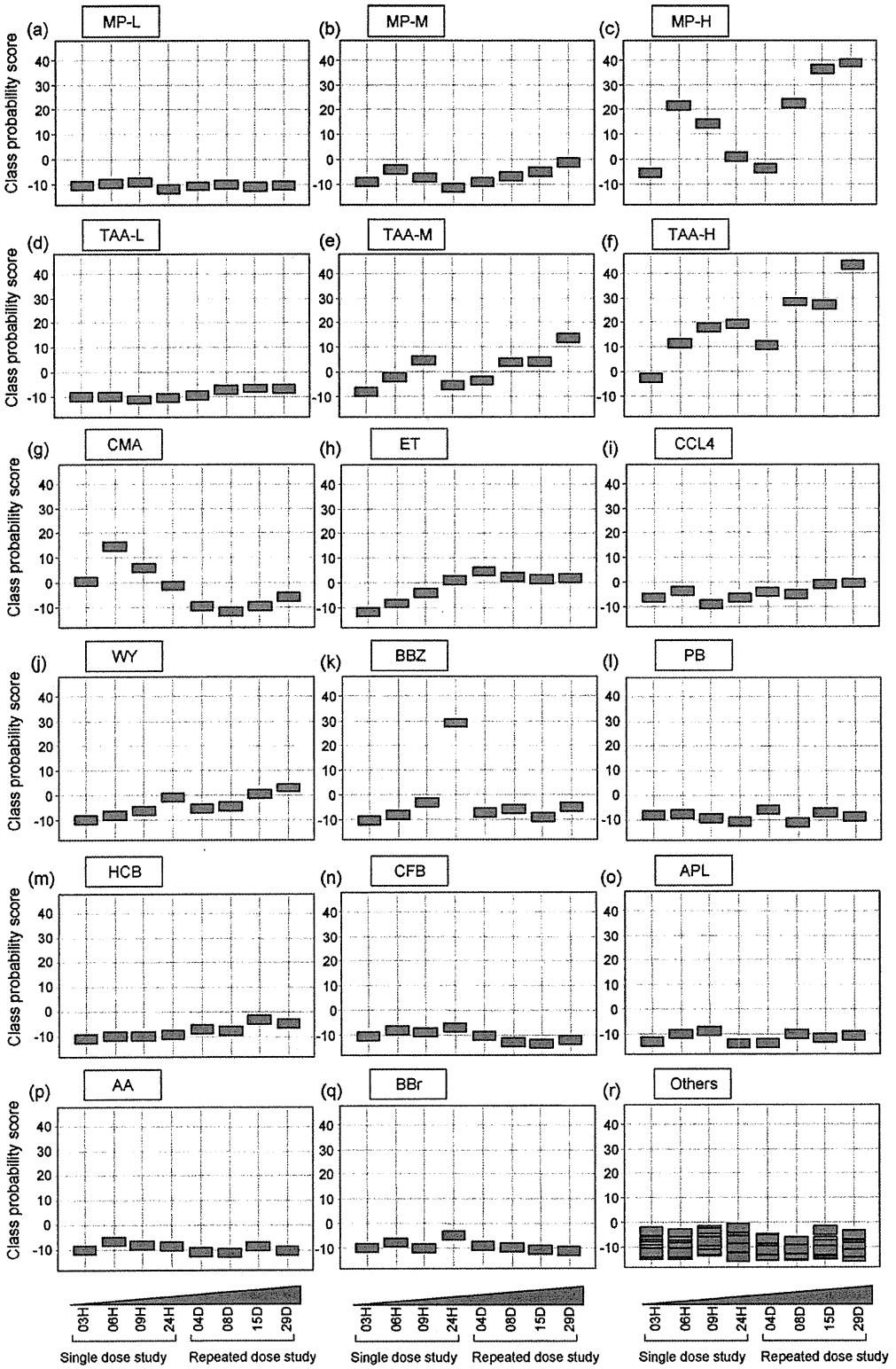

Fig. 4. PAM prediction score. The PAM class probability was converted to a score as described in Section 2 in order to enable quantitative comparison. The score is shown for MP ((a) 10 mg/kg, L; (b) 30 mg/kg, M; (c) 100 mg/kg, H), TAA ((d) 4.5 mg/kg, L; (e) 15 mg/kg, M; (f) 45 mg/kg, H), CMA ((g) 150 mg/kg), ET ((h) 250 mg/kg), CCL4 ((i) 300 mg/kg), WY ((j) 100 mg/kg), BBZ ((k) 300 mg/kg), PB ((l) 100 mg/kg), HCB ((m) 300 mg/kg), CFB ((n) 300 mg/kg), APL ((o) 150 mg/kg), AA ((p) 30 mg/kg), BBr ((q) 200 mg/kg), and (r) the other 17 chemicals. For abbreviation of the compounds, see Table 1.